Supporting Information for

The Transition Metal-Catalyzed [π2s + π2s + σ2s + σ2s] Pericyclic Reaction: Woodward–Hoffmann Rules, Aromaticity, and Electron Flow.

Alexander Q. Cusumano,[†] William A. Goddard, III,*[,††] and Brian M. Stoltz,*[,†]

[†]Warren and Katharine Schlinger Laboratory of Chemistry and Chemical Engineering, Division of Chemistry and Chemical Engineering, California Institute of Technology, Pasadena, California 91125, United States

[††] Materials and Process Simulation Center, Beckman Institute, California Institute of Technology, Pasadena, California 91125, United States.

wag@caltech.edu

stoltz@caltech.edu

Table of Contents:

General Computational Details

All quantum mechanical calculations were performed with ORCA version 4.1 and 4.2.[1] Geometries of open-shell species (**TS5**, **10**, and **TS6**) and their precursors (**3**, **4** and **5**) were optimized with complete active space self-consistent field (CASSCF) theory. The active space was defined as the correlating valence electrons and orbitals as obtained by the corresponding orbital correlation diagrams (see below). The triple ζ quality def2-TZVP basis set[2] was used on all atoms. Further details on choice of active spaces are provided below. Results obtained via broken-symmetry density functional theory (BS-DFT) are provided below for comparison. For transition metal complexes with insignificant multiconfigurational character (**6**, **7**, **TS3**, **TS4**, **8**, and **9**), geometries were obtained from dispersion-corrected DFT. The PBE0 global hybrid density functional[3] paired with Becke–Johnson damped D3 dispersion corrections[4] (henceforth referred to as PBE0-D3(BJ)) and the def2-TZVP basis set on all atoms was employed. The small-core def2-ECP pseudopotential[5] was used on Pd – i.e. 18 explicit electrons including the 4s and 4p core shells were defined.

To account for dynamical correlation, N-electron valence state perturbation theory [6] (NEVPT2) single point calculations were carried out on all stationary points (CASSCF and DFT geometries) from the corresponding CAS references. The strongly contracted variant of NEVPT2 was employed. Control calculations with quasi-degenerate NEVPT2 (QD-NEVPT2) [7] provided indistinguishable results from that of the strongly contracted method. Thus, the inclusion of dynamical correlation did not significantly alter the CI coefficients of the CASSCF wavefunction for the states of interest. Solvation was accounted for in these single point calculations with the SMD model for THF.[8] In addition to single point calculations with NEVPT2/def2-TZVPP/SMD(THF), for the compounds that were optimized with PBE0-D3(BJ)/def2-TZVP, additional single point calculations were carried out with PBE0-D3(BJ)/def2-TZVP/SMD(THF) for comparison.

Thermal corrections were obtained from the unscaled vibrational frequencies computed at the level of theory employed for geometry optimization. The Quasi-RRHO method[9] was applied to correct for the breakdown of the harmonic oscillator approximation in low frequency vibrations. For CASSCF and DFT calculations these frequencies were computed numerically and analytically, respectively. All stationary points were characterized by the appropriate number of imaginary vibrational modes (zero for optimized geometries and one for transition states). Intrinsic reaction coordinate (IRC) analyses were carried out to ensure all transition states connect saddle points to the

appropriate minima. Conformer searching was carried out manually and energies reported are from lowest energy conformers. All energies reported in the manuscript are free energies calculated at 298.15 K and at a 1 atm standard state. Applying thermal corrections obtained at the optimization level of theory to the single point electronic energies (and solvation free energies), final Gibbs free energies are accordingly:

$$G_{solv} = E(el)^{SP} + ZPE + E(vib) + E(rot) + E(trans) + k_bT - TS + \Delta G(solv)^{SP}$$

The resolution of identity (RI) and chain-of-spheres[10] (keyword = RIJCOSX) approximations were utilized for coulomb and exchange integrals, respectively. Automatic generation of auxiliary basis sets was employed (keyword = AutoAux).[11] [Note that in geometry optimization, frequency, and IRC calculations with CASSCF, the RI and COS approximations were not used as they are not implemented with analytical (nuclear) gradients in ORCA version 4.2.0]. The finest integration grid settings (Grid7, GridX9, NoFinalGrid) were utilized in all calculations.

NEVPT2/CASSCF Active Spaces and Results

Unless otherwise specified, energies provided below are solvated CASSCF and NEVPT2 free energies (in Hartree) with the def2-TZVP basis set and SMD implicit solvation model for THF. Energies further refined with the def2-TZVPP basis set are provided in the text and supporting excel document (nearly identical results were obtained). Weights (C_i^2) of the three configurations with the largest contributions to the ground state CI coefficient vector are provided. The notation [2200] corresponds to a configuration with double occupancy of the first and second MOs of the active space and zero occupancy of the third and fourth active space MOs. Unless otherwise noted, active space MOs are depicted as the natural orbitals of the CAS wavefunction and are rendered with a contour value of 0.07. Active spaces were chosen to include the correlating valence orbitals as determined by the corresponding Woodward–Hoffmann orbital correlation diagrams.[12] The active space may be localized to confirm the correct active space compositions. Unless otherwise specified, state-averaging was not employed, and results are that of the lowest energy singlet state. Occupancy numbers are provided in parentheses next to MO numbers. Orbital energy eigenvalues (from NEVPT2) are listed when the ordering of the active space MOs by occupancy number is different than the ordering by energies.

Complex **1**:

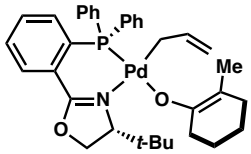

1

CASSCF(8,8)	-2022.394386
NEVPT2(8,8)	-2030.146571
Weight	**Configuration**
0.87749	[22220000]
0.02871	[21211010]
0.02357	[22020200]

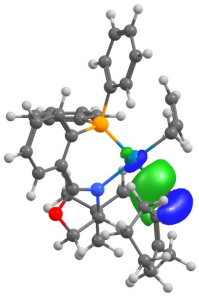

MO150 (1.98)

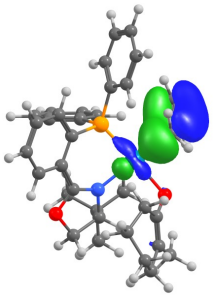

MO151 (1.93)

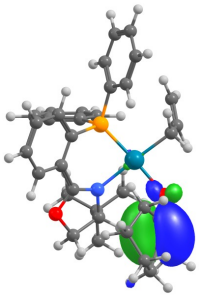

MO152 (1.93)

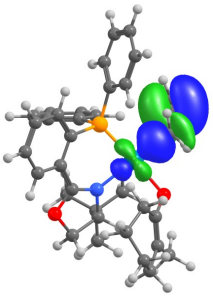

MO153 (1.90)

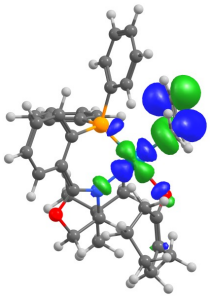

MO154 (0.10)

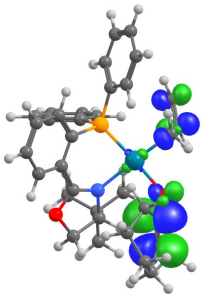

MO155 (0.07)

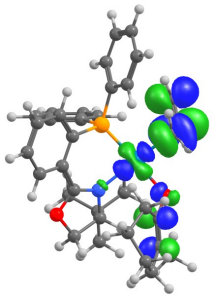

MO156 (0.07)

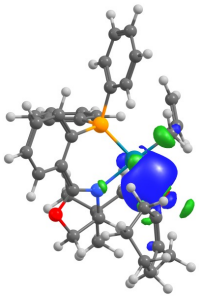

MO157 (0.02)

Figure S1. *Geometry taken from reference 13 (BP86-D3/LANL2TZ(f)[Pd],6-31G(d)). Energies above are CASSCF and NEVPT2 solvated electronic energies in Hartree. Orbital energy eigenvalues (by ascending MO) in eV: –0.5516, –0.4294, –0.2868, –0.3067, 0.1907, 0.3014, 0.3116, 0.9729. Isosurface level adjusted to 0.03 for ease of visualization.*

Transition state **TS1**:

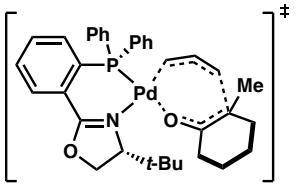

TS1

CASSCF(8,8)	-2022.358794
NEVPT2(8,8)	-2030.135158
Weight	**Configuration**
0.85071	[22220000]
0.03808	[22202000]
0.00849	[22111100]

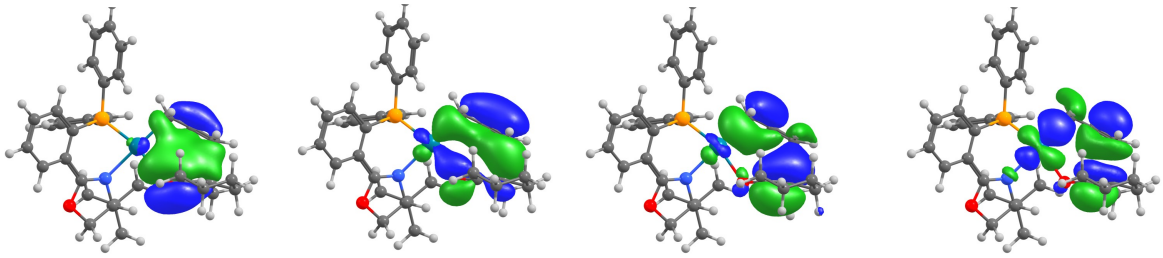

MO150 (1.97) **MO151** (1.94) **MO152** (1.93) **MO153** (1.85)

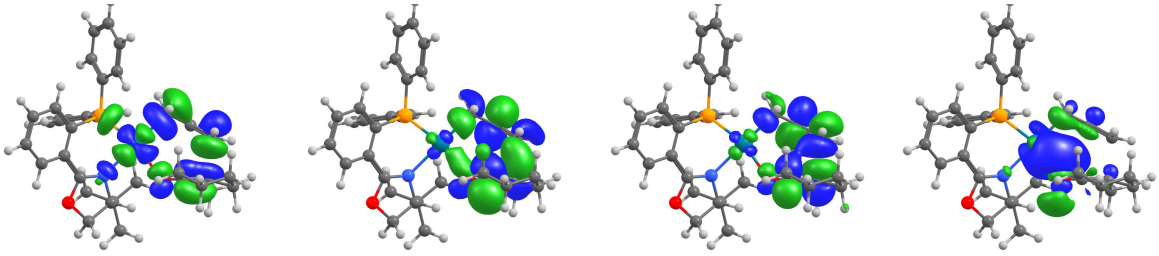

MO154 (0.14) **MO155** (0.10) **MO156** (0.06) **MO157** (0.02)

Figure S2. *Geometry taken from reference 13 (BP86-D3/LANL2TZ(f)[Pd],6-31G(d)). Energies above are CASSCF and NEVPT2 solvated electronic energies in Hartree. Orbital energy eigenvalues (by ascending MO) in eV: –0.5101, –0.4084, –0.3196, –0.2322, 0.1617, 0.2167, 0.3781, 0.7215. Isosurface level adjusted to 0.04 for ease of visualization.*

Complex **2**:

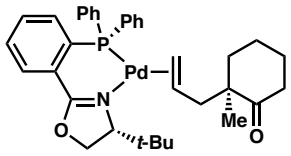

2

CASSCF(8,8)	-2022.420396
NEVPT2(8,8)	-2030.191318
Weight	Configuration
0.90785	[22220000]
0.02896	[22020200]
0.02830	[22202000]

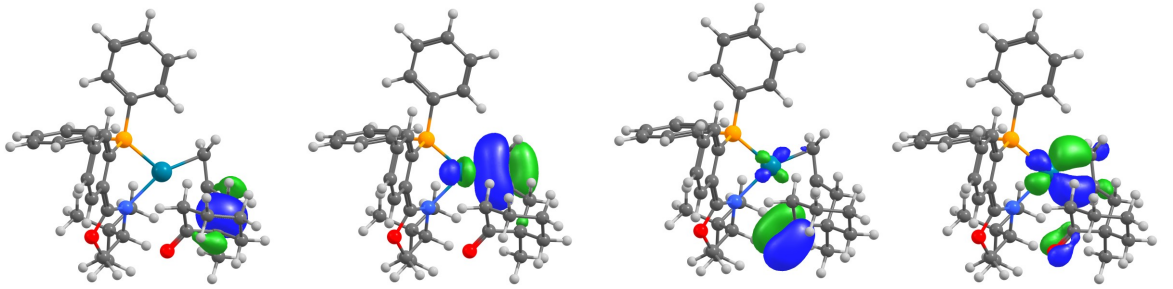

MO150 (1.98) **MO151** (1.97) **MO152** (1.93) **MO153** (1.92)

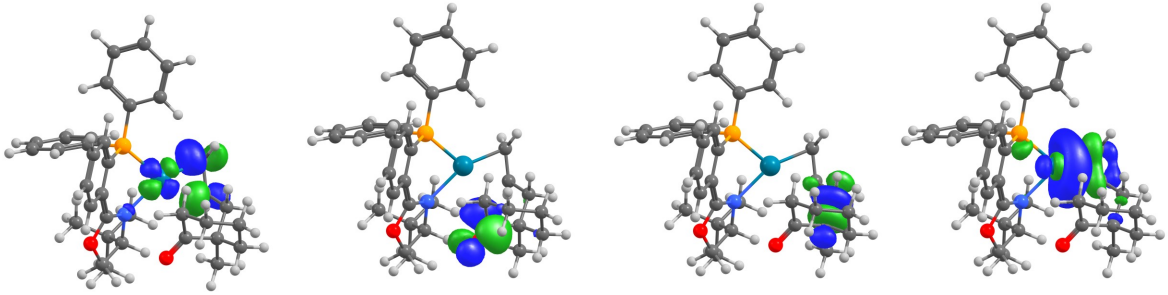

MO154 (0.09) **MO155** (0.07) **MO156** (0.02) **MO157** (0.02)

Figure S3. *Geometry taken from reference 13 (BP86-D3/LANL2TZ(f)[Pd],6-31G(d)). Energies above are CASSCF and NEVPT2 solvated electronic energies in Hartree. Orbital energy eigenvalues (by ascending MO) in eV: –0.6097, –0.4323, –0.4795, –0.3032, 0.2540, 0.2951, 0.7745, 0.5139. Isosurface level adjusted to 0.04 for ease of visualization.*

Diallyl sulfone **3**:

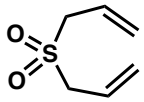

3

CASSCF(8,8)	-780.349971
NEVPT2(8,8)	-782.106985
Weight	Configuration
0.90106	[22220000]
0.03843	[22111100]
0.01005	[22202000]

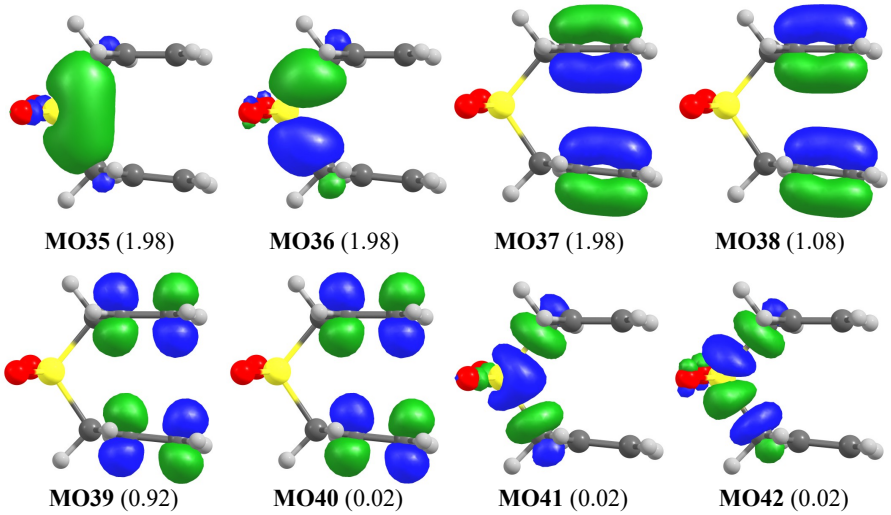

Figure S4. Active space orbitals for compound **3**.

Transition state **TS5**:

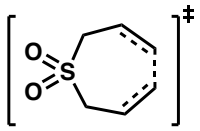

TS5

CASSCF(8,8)	-780.258382
NEVPT2(8,8)	-782.031183
Weight	Configuration
0.68584	[22220000]
0.26002	[22202000]
0.01996	[22111100]

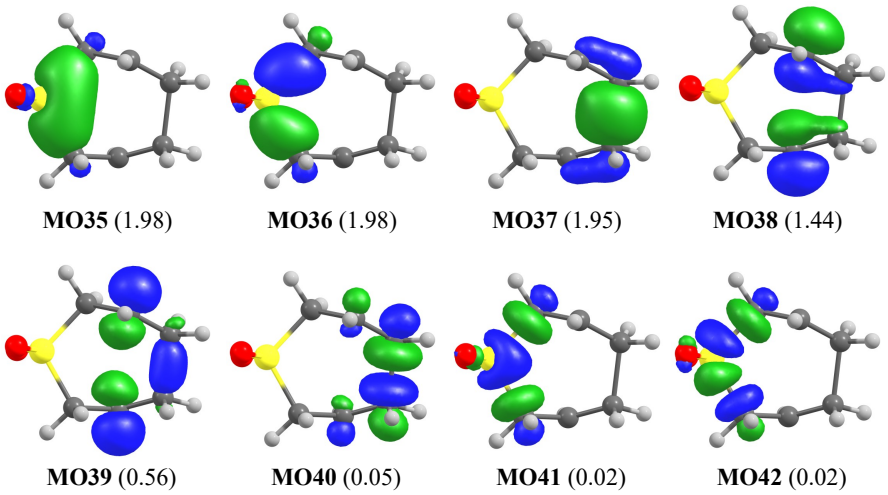

Figure S5. Active space orbitals for compound **TS5**.

Diradical **10**:

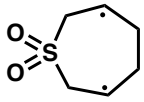

10

CASSCF(8,8)	-780.261600
NEVPT2(8,8)	-782.026896
Weight	Configuration
0.52173	[22220000]
0.44492	[22202000]
0.00405	[12120101]

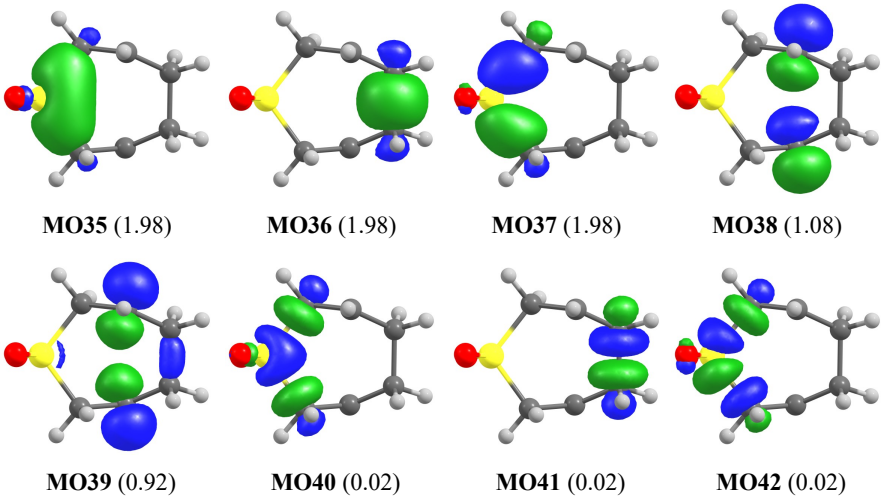

Figure S6. Active space orbitals for compound **10**.

Transition state **TS6**:

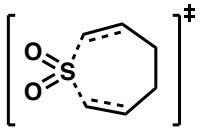

TS6

CASSCF(8,8)	-780.244658
NEVPT2(8,8)	-782.024561
Weight	Configuration
0.61644	[22220000]
0.29502	[22202000]
0.04355	[22111100]

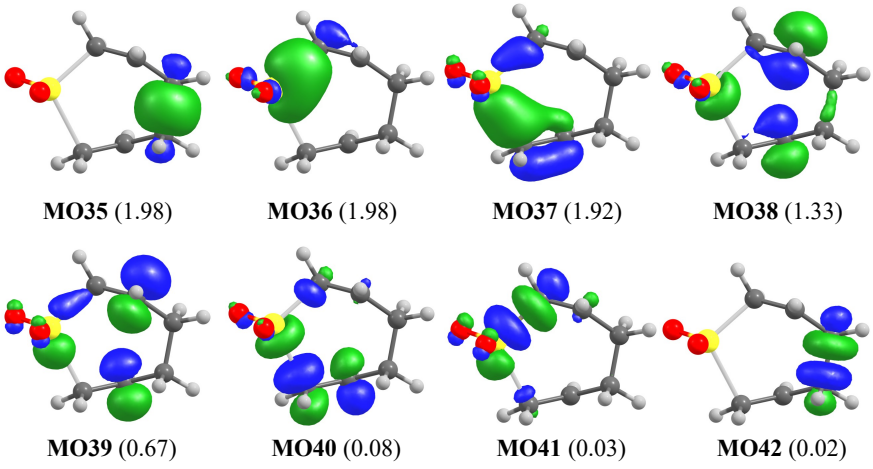

Figure S7. Active space orbitals for compound **TS6**.

SO_2 **4**:

4

CASSCF(2,2)	-547.345604
NEVPT2(2,2)	-548.090971
Weight	Configuration
0.98002	[20]
0.01998	[02]

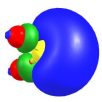

MO15 (1.96)

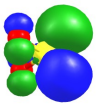

MO16 (0.04)

Figure S8. Active space orbitals for compound **4**.

(s-cis)-1,5-hexadiene **5**:

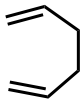

5_cis

CASSCF(6,6)	-233.022382
NEVPT2(6,6)	-234.026032

Weight	Configuration
0.91161	[222000]
0.03853	[211110]
0.01066	[220200]

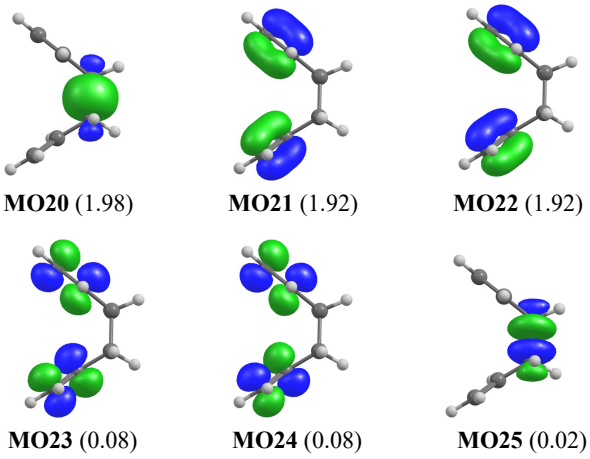

Figure S9. Active space orbitals for compound **5**. *(Not visible at isosurface printed above: MO23 and MO24 experience slight mixing with MO25 and MO20, respectively, such that the resulting orbital energy eigenvalue for MO23 is lower than that of the symmetric MO24 (0.2332 eV and 0.2374 eV).*

(s-trans)-1,5-hexadiene **5_trans**:

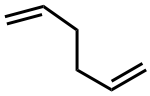

5_trans

CASSCF(6,6)	-233.004232
NEVPT2(6,6)	-234.022461
Weight	Configuration
0.92057	[222000]
0.03724	[211110]
0.00985	[202200]

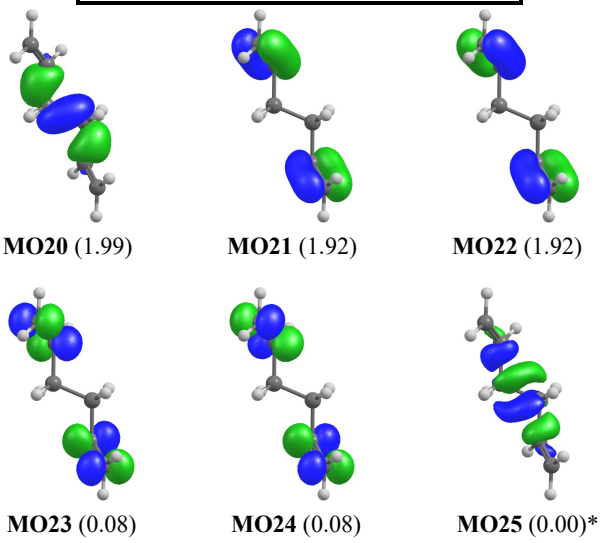

Figure S10. Active space orbitals for compound **5_trans**. **Occupancy 0.00465*

Complex **6**:

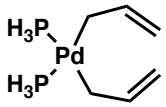

6

CASSCF(8,8)	-1044.976965
NEVPT2(8,8)	-1047.103294
Weight	Configuration
0.88527	[22220000]
0.01649	[22111100]
0.01002	[21211010]

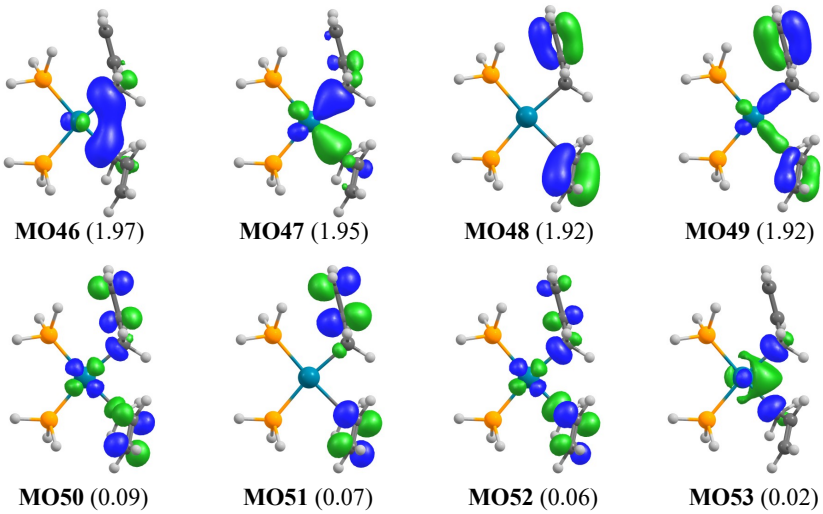

Figure S11. Active space orbitals for compound **6**. *Orbital energy eigenvalues (by ascending MO) in eV: –0.4110, –0.4486, –0.3197, –0.3230, 0.1931, 0.2702, 0.3169, 0.6241. In this conformation, the antisymmetric Pd–L σ* and the antisymmetric C–C π* symmetry adapted linear combinations mix to give rise to MO50 and MO52.*

Complex **7**:

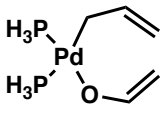

7

CASSCF(8,8)	-1080.874182
NEVPT2(8,8)	-1083.041153
Weight	Configuration
0.88716	[22220000]
0.03125	[22111100]
0.02575	[20220020]

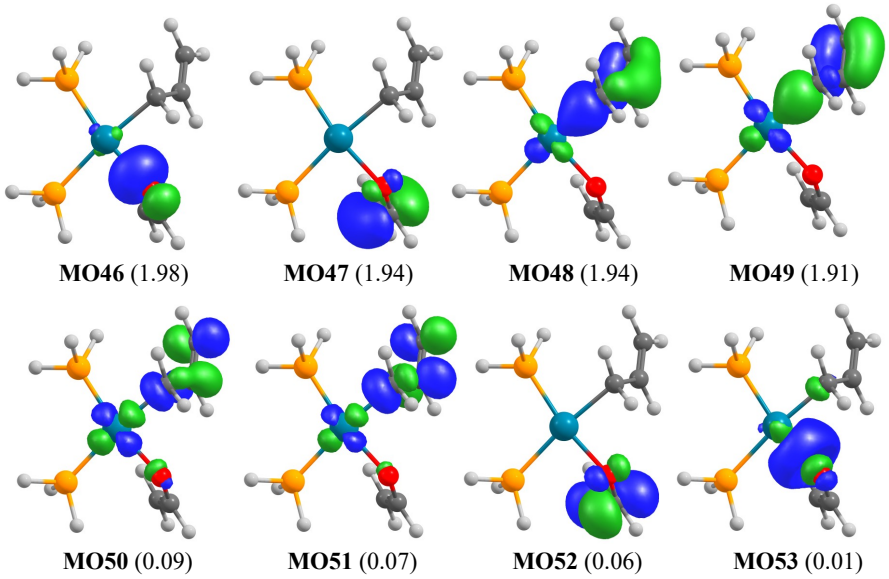

Figure S12. Active space orbitals for compound **7**. *Orbital energy eigenvalues (by ascending MO) in eV: –0.5622, –0.3144, –0.4403, –0.3213, 0.1826, 0.2975, 0.2983, 0.9742. In this conformation, the* n^1*-allyl ligand C–C p orbitals are nearly coplanar and further mix with the Pd-based* $d_{x^2-y^2}$ *(MO48–MO51). If the active space is localized (Foster–Boys) the C–C* π/π^* *and Pd–C* σ/σ^* *may be separated for ease of interpretation.*

Transition state **TS3**:

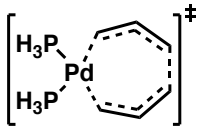

TS3

CASSCF(8,8)	-1044.936576
NEVPT2(8,8)	-1047.082378
Weight	Configuration
0.85693	[22220000]
0.01682	[22202000]
0.01094	[22111100]

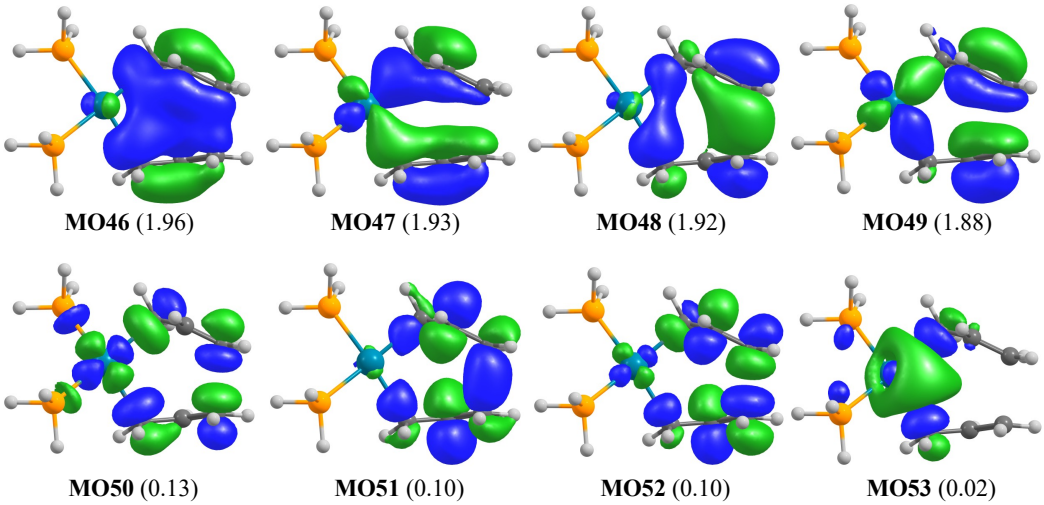

Figure S13. Active space orbitals for compound **TS3**. *Isosurface value adjusted to 0.04 for ease of visualization. Orbital energy eigenvalues (by ascending MO) in eV: –0.4443, –0.4016, –0.3064, –0.2400, 0.1574, 0.2046, 0.3684, 0.5126.*

Transition state **TS4**:

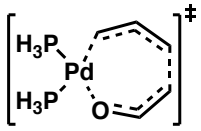

TS4

CASSCF(8,8)	-1080.838314
NEVPT2(8,8)	-1083.018807
Weight	Configuration
0.86058	[22220000]
0.03715	[22202000]
0.00724	[22020200]

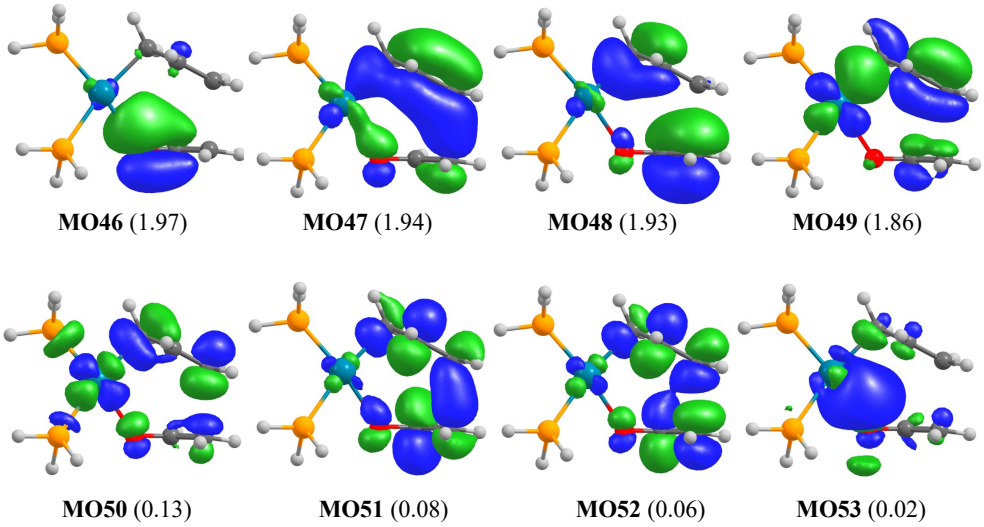

Figure S14. Active space orbitals for compound **TS4**. *Isosurface value adjusted to 0.04 for ease of visualization. Orbital energy eigenvalues (by ascending MO) in eV: –0.5448, –0.4209, –0.3126, –0.2783, 0.1404, 0.2406, 0.3519, 0.7700.*

Complex **8**:

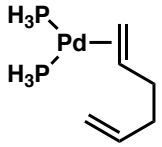

8

CASSCF(8,8)	-1045.009114
NEVPT2(8,8)	-1047.148494
Weight	Configuration
0.88527	[22220000]
0.01649	[22111100]
0.01002	[21211010]

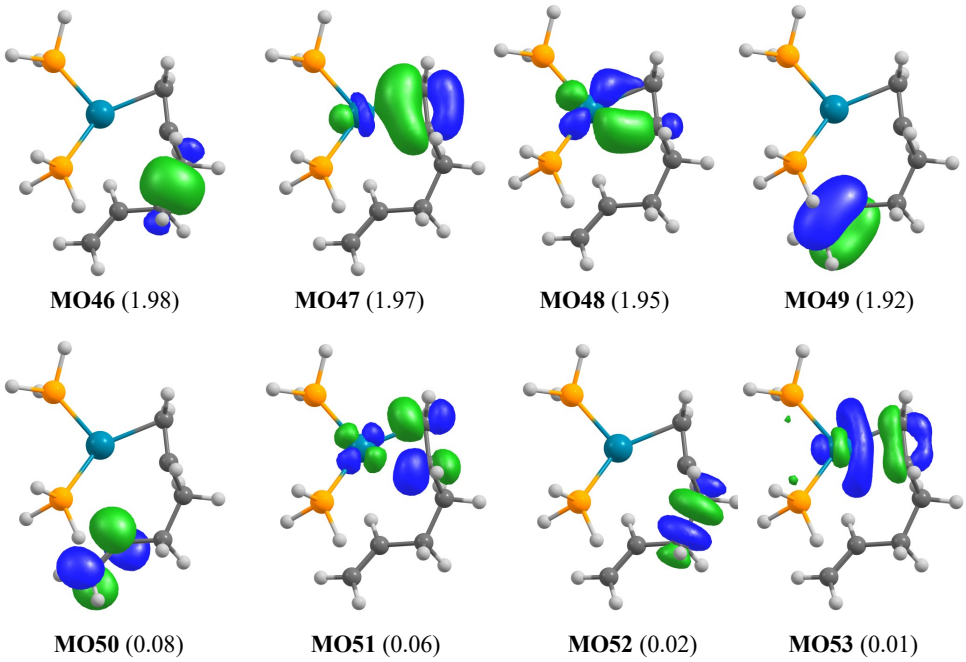

Figure S15. Active space orbitals for compound **8**. *Isosurface value adjusted to 0.04 for ease of visualization. Orbital energy eigenvalues (by ascending MO) in eV: –0.6193, –0.4392, –0.3288, –0.3509, 0.2247, 0.2579, 0.8061, 0.4683.*

Complex **9**:

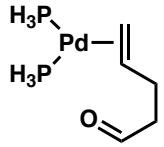

9

CASSCF(8,8)	-1080.909107
NEVPT2(8,8)	-1083.101216
Weight	Configuration
0.92253	[22220000]
0.02687	[22202000]
0.01400	[22020200]

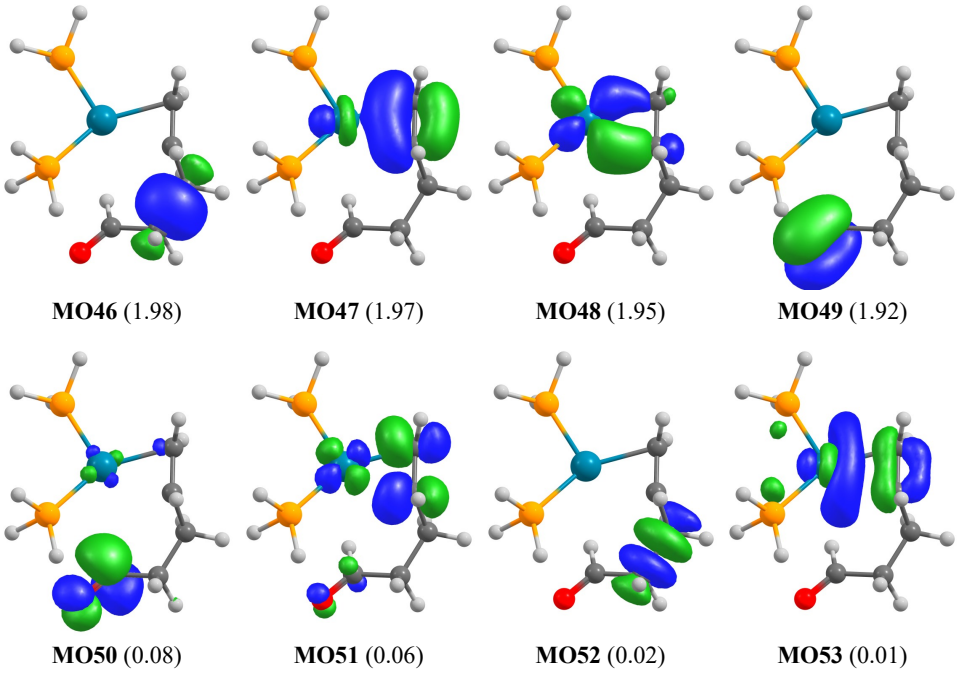

Figure S16. Active space orbitals for compound **9**. *Isosurface value adjusted to 0.06 for ease of visualization. Orbital energy eigenvalues (by ascending MO) in eV: –0.6342, –0.4444, –0.3324, –0.5055, 0.2854, 0.2572, 0.8066, 0.4687.*

Additional Notes on CASSCF/NEVPT2 Calculations

The frozen core approximation was not used in the NEVPT2 calculations (keyword: "! NoFrozenCore"). Solvated free energies include the cavitation, dispersion, structure (CDS) terms as calculated in the SMD model.[8]

Practical note to users: For efficiently converging active spaces with weakly correlated valence-bond-like orbitals (such as the C–C(σ/σ*) in the starting complexes and products), we recommend use of the PMO virtual orbital optimization feature in ORCA. A standard procedure involved converging the MCSCF with an active space excluding the weakly correlating pair, localization of the internal space, locating the valence bond orbital of interest, then optimization of a corresponding virtual orbital (using the PMO methodology (RefMO)). Generally, expanding the active space to include the natural orbital-like pair affords smoothly convergence of the MCSCF.

Discussion on Other Main Group Chelefuges

In our investigation of the [π2s + π2s + σ2s + σ2s] reaction, we employ diallyl sulfone (**3**) as a main group analog to bis(η^1-allyl)Pd(PH_3)$_2$ complex **6**. In addition to SO_2, CO and N_2 are also viable main group chelefuges. Thus, the [π2s + π2s + σ2s + σ2s] reactions of hepta-1,6-dien-4-one or diallyl isodiazene may be considered. For these scenarios, there are *nine* correlating valence orbitals – occupied by 10 valence electrons (see Chapter 3 of reference 12). Both reactions are similarly symmetry forbidden. As a representative example, the orbital correlation diagram for the reaction of hepta-1,6-dien-4-one to CO and 1,5-hexadiene is provided below (Figure S17). In the general [π2s + π2s + σ2s + σ2a] reaction, we only consider linear departure/approach of the chelefuge due to the geometric/steric constraints of the seven-membered transition state. An exception to this may be methylene carbene, which could possibly undergo the thermally allowed [π2s + π2s + σ2s + σ2a]/[ω2a + π2s + π2s + σ2s] reaction, i.e. with non-linear departure/approach of the carbene.

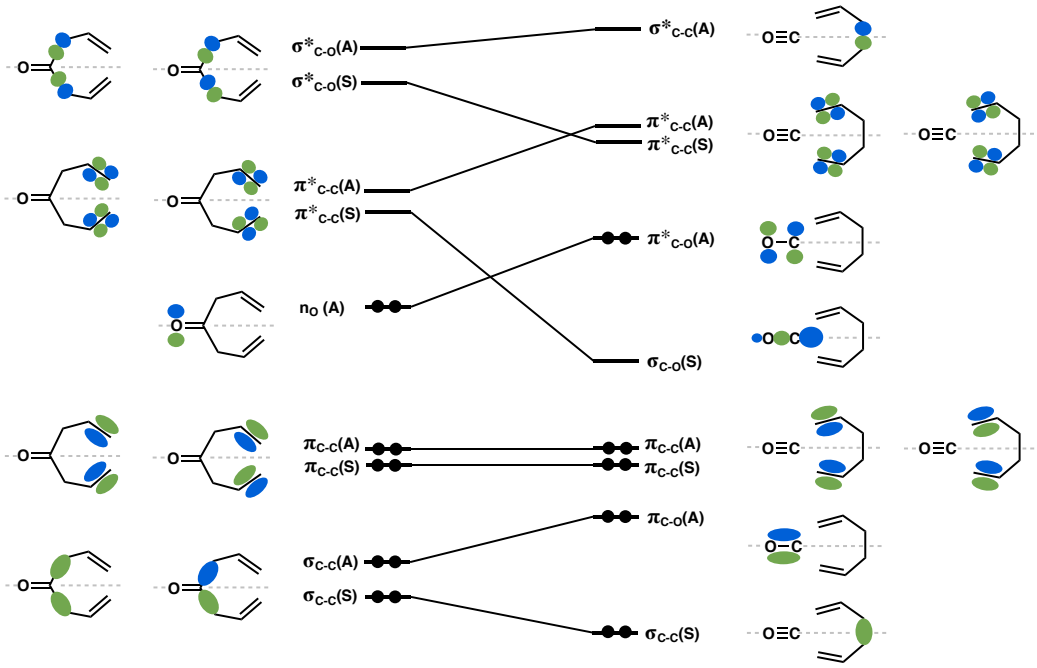

Figure S17. Orbital correlation diagram for the ground state symmetry-forbidden [π2s + π2s + σ2s + σ2s] extrusion of CO from hepta-1,6-dien-4-one.

Exploring Exchange Coupling in Diradical 10

The RI and COS integral approximations were not used in calculations evaluating exchange coupling. All computations were carried out in the gas phase. State averaging over the relevant singlet and triplet diradical states was employed in CASSCF calculations. Results obtained with the minimal (2,2) active space, i.e. including only the local spin centers, are provided for comparison. Hypothetical diradical species **10** is a metastable intermediate on the singlet CAS(8,8) and BS-DFT ($M_s = 0$) potential energy surfaces. In the case of BS-DFT, the diradical was found as an intermediate regardless of choice of functional ((U)PBE0-D3(BJ), (U)PBE-D3(BJ), (U)M06-2X).[14]

Exchange coupling interaction may be described through the phenomenological Heisenberg–Dirac–van Vleck Hamiltonian[15]:

$$\hat{H}_{\mathrm{HDvV}} = -2J\hat{S}_A\hat{S}_B$$

where $\hat{S}_A$ and $\hat{S}_B$ are "local" spin operators on spin sites A and B. J is defined as the exchange coupling constant. Thus, for the coupling of two spin-1/2 magnetic sites, J is expressed as:

$$J = -\frac{1}{2}(E_T - E_S)$$

where E_T and E_S are the energies of the triplet- and singlet-coupled diradical states, respectively. When $J > 0$, i.e. $E_T < E_S$, the interaction is termed ferromagnetic. Likewise, $J < 0$ implies an antiferromagnetic coupling of the two spins. As a consequence of a single determinant formulation, the broken-symmetry DFT solution of an open-shelled singlet state is a mixture of the $M_s = 0$ singlet and triplet states.[16] Thus, calculation of exchange coupling was performed after removal of spin contamination. The spin projection to the "true" singlet energy was carried out via the Yamaguchi equation[17]:

$$E_T - E_S = \frac{2}{\langle S^2 \rangle_T - \langle S^2 \rangle_{BS}} (E_T - E_{BS})$$

As such, the *J* values we report via BS-DFT are calculated as:

$$J = -\frac{E_T - E_{BS}}{\langle S^2 \rangle_T - \langle S^2 \rangle_{BS}}$$

Single point calculations with SA-CAS(8,8) on the CAS(8,8) PES initially suggest an antiferromagnetic coupling between the two spin-1/2 centers (J = –12.1 cm^{-1}) of **10**. However, inclusion of dynamical correlation via SC-NEVPT2, with the SA-CAS(8,8) reference, reveals a weak ferromagnetic coupling (J = 3.2 cm^{-1}) (Table 1, entry 5). BS-DFT single point calculations carried out on the CAS(8,8) geometry also suggest a singlet-coupled diradical, with J = –38.9 cm^{-1}. Conversely, DFT single point calculations at both the high spin and broken-symmetry (BS-)DFT-optimized geometries suggest ferromagnetism (Table S1, entries 9 and 10). Unsurprisingly, these data suggest the treatment of dynamical electron correlation is crucial in obtaining qualitatively meaningful results.

Table S1. Calculation of spin exchange coupling constant (*J*) between spin centers in 1,4-diradical 10.[a]

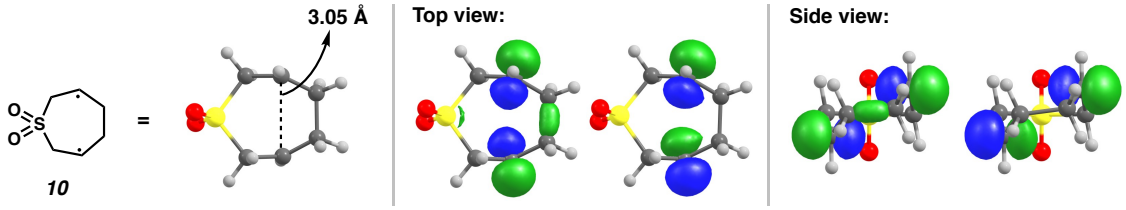

Entry No.	Method	J (cm^{-1})
1	SA-CAS(2,2)	59.1
2	SA-CAS(8,8)	–12.1
3	SC-NEVPT2/SA-CAS(2,2)	–14.1
4	FIC-NEVPT2/SA-CAS(2,2)	–14.0
5	SC-NEVPT2/SA-CAS(8,8)	3.2
6	FIC-NEVPT2/SA-CAS(8,8)	7.0
7	**IDDCI**[b]	**82.9**
8	(U)PBE0-D3(BJ)[c]	–38.9
9	(U)PBE0-D3(BJ)[d]	30.0
10	(U)PBE0-D3(BJ)[e]	37.0

[a] Unless otherwise noted, performed on the singlet CAS(8,8)/def2-TZVP geometry **10**. All calculations above employ the def2-TZVP basis set on all atoms, no integral approximations, and are carried out in the gas phase. Pictured above are the two natural orbitals in the CAS(8,8) active space describing bonding and antibonding pairing in diradical **10**. [b] IDDCI (see below) starting from the SA-CAS(2,2) wavefunction. [c] BS-DFT single point calculation on CAS(8,8)/def2-TZVP geometry. [d] Single point calculation on broken-symmetry ($M_S = 0$) (U)PBE0-D3(BJ)/def2-TZVP optimized geometry. [e] Single point calculation on high spin ($S = 1$) (U)PBE0-D3(BJ)/def2-TZVP optimized geometry.

For a more rigorous treatment of static and dynamic correlation, multireference calculations were carried out with the Iterative Difference Dedicated Configuration Interaction (IDDCI) method.[18] The standard DDCI approach resembles that of an uncontracted MRCI (singles and doubles), where completely inactive double excitations are omitted. The reference states were defined to be the singlet and triplet diradical states. The state-averaged CAS(2,2) wavefunction was taken to be the initial orbitals. The results obtained with DDCI are highly depended on the choice of reference orbitals. To help alleviate this starting orbital dependence and generally obtain more accurate results, we employed the Iterative DDCI method (IDDCI) of Malrieu and coworkers.[11b] In IDDCI, an iterative MO improvement strategy is utilized in which a DDCI calculation is first converged, followed by construction of the state-averaged single-particle density matrix and diagonalization to give a set of

new set of state-averaged natural orbital-like MOs. These MOs then serve as the starting orbital basis for a subsequent DDCI calculation. The process is repeated until self-consistency (i.e. the energies of the states stabilize).

As implemented in the ORCA program, convergence of the calculated exchange coupling constant and state energies is achieved with the parameters $T_{sel} = 1x10^{-11}$ (default $1x10^{-6}$) and $T_{pre} = 1x10^{-4}$ (default $1x10^{-4}$). A sample input for the IDDCI calculation is provided below:

```
! def2-TZVP NoPop Grid7 NoFinalGrid
! MORead VeryTightSCF NoIter AllowRHF

%base "SampleName"
%moinp "SampleStart.gbw"
%method
FrozenCore fc_ewin
end

%mrci
        EWin -10,1000
        CIType MRDDCI3
        Solver DIIS
        UseIVOs true
        Tsel 1e-11
        Tpre 1e-5
        AllSingles true
        DavidsonOpt none
        NatOrbIters 5
        NewBlock 1 *
          NRoots 1
          refs cas(2,2) end
          end
        NewBlock 3 *
          NRoots 1
          refs cas(2,2) end
          end
end

* xyzfile 0 1 Sample.xyz
```

Due to the rapidly increase in computational cost with increase in the size of the active space, we elected to employ the (2,2) active space consisting of the two local magnetic orbitals. Calculations with the (8,8) active space were explored; however, it was found that convergence of the exchange coupling constant and state energies was not fully achieved with values of T_{sel} that yield a reasonable computational cost. Thus, we suggest the results obtained from the tightly converged (2,2) active space to be more robust. *Note that the results are qualitatively similar regardless – both (2,2) and (8,8) active spaces afford $J > 0$.* After five iterations, the IDDCI(2,2) method converges to an

exchange coupling constant of 82.9 cm^{-1} (Figure S18). These results are in accord with that of NEVPT2(8,8) and BS-DFT, suggesting a triplet ground state of diradical **10**.

In summary, the concerted ground state [π2s + π2s + σ2s + σ2s] reaction of diallyl sulfone **3** to SO_2 (**4**) and 1,5-hexadiene (**5**) is symmetry forbidden. Owing to the triplet ground state of diradical **10**, the individual steps of the stepwise mechanism are formally spin forbidden — granted the singlet and triplet states are nearly degenerate (ΔE_{T-S} of *ca.* 0.5 kcal/mol) in the weakly coupled diradical.

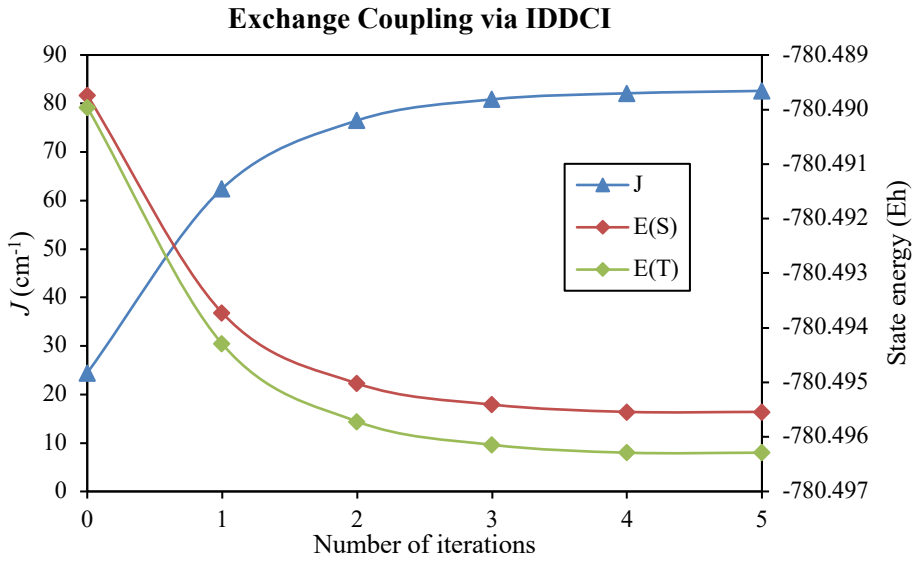

Figure S18. Convergence of exchange coupling and state energies via iterative MO optimization in DDCI (IDDCI).

Redox Innocence of the PHOX Ligand in the [π2s + π2s + σ2s + σ2s] Reaction

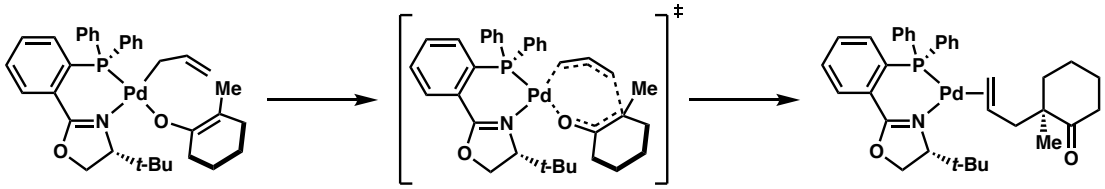

1 ***TS1*** ***2***

The general Pd-catalyzed [π2s + π2s + σ2s + σ2s] pericyclic reaction is symmetry allowed without mandatory implication of ligand-based excited states/configurations. However, in the case of Pd(PHOX) complexes, we sought to evaluate whether the π system of the PHOX ligand is capable of facilitating the reductive elimination through ligand-based redox activity. First, we note that the ground state densities obtained with PBE0-D3(BJ)/def2-TZVP are stable with respect to spin symmetry breaking. Thus, at the DFT level, the ground state along the reaction path **1** → **TS1** → **2** is

well represented as a closed-shell singlet (CSS). Time-dependent density functional theory (TD-DFT) calculations were then carried out on stationary points **1**, **TS1**, and **2** at the PBE0-D3(BJ)/def2-TZVP/SMD(THF) level of theory. The TD-DFT calculations suggest no low energy excited states along the ground state PES. The lowest of these vertical transitions is that of the ^{3}(M/L→L) at **TS1**, which is calculated to be nearly 1.0 eV (Table S2). All other excitations (M→M, L→M/L, etc.) are found to be > 2 eV. The PHOX π*-based LUMO (Figure S19) serves as a common acceptor in each of the lowest energy transitions in Table 2. These results suggest that redox contribution of the PHOX ligand along the ground state PES is likely trivial.

Table S2. Lowest energy TD-DFT vertical excitations at stationary points 1, TS1, and 2.[a]

	1		**TS1**		**2**	
	Excitation	Energy (eV)	Excitation	Energy (eV)	Excitation	Energy (eV)
Singlet	L → L	1.463	M/L → L	1.401	MLCT	2.264
Triplet	L → L	1.014	M/L → L	0.986	MLCT	1.941

[a] TD-DFT vertical excitations with PBE0-D3(BJ)/def2-TZVP/SMD(THF) and adapted triplets from the RKS reference. L = ligand, M = metal, M/L = mixed metal/ligand.

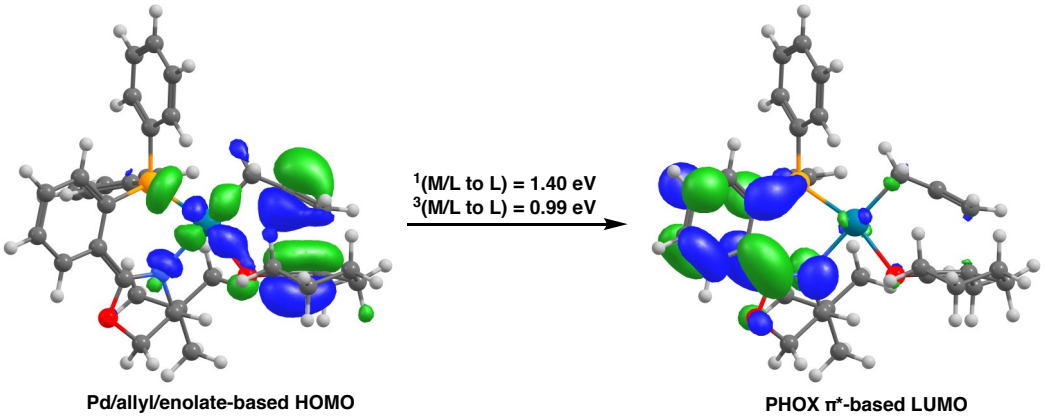

Figure S19. Orbitals involved in the vertical transitions to the lowest energy singlet and triplet excited states at **TS1**.

Nucleus Independent Chemical Shift Calculations

Calculations of Nucleus Independent Chemical Shift (NICS) were carried out in order to probe the aromatic character of **TS3**. In this investigation, the formalism of Schleyer and coworkers is followed.[19] Reported NICS values are the negative of the calculated isotropic chemical shift/shielding at the geometric center of the ring in question. These calculations were carried out with the NMR module in ORCA. Calculations of NICS were conducted in the gas phase at the PBE0-D3(BJ)/def2-TZVP level of theory. Gauge independent atomic orbitals (GIAO) were used and the relevant one-electron and two-electron integrals were evaluated analytically and with the RIJK approximation, respectively. A ghost atom ("H:", no nuclear charge nor electrons) was used to define a point in space at which shielding was to be determined. A highly contracted basis (and auxiliary basis) function was then assigned to the ghost atom. *This procedure was used to ensure the proper grid points were assigned to the point in space without significantly perturbing the ground state density*. *Note that the results are independent of the chosen exponent as long as the exponent is large*. For example, the following would be added to the geometry block of an input file to define a point with cartesian coordinates (0.0000, 1.0000, 2.0000):

```
H:    0.0000   1.0000   2.0000   newgto S 1 1 1000000 1 end newauxJKgto S 1 1 2000000 1 end
```

At the PBE0-D3(BJ)/def2-TZVP level of theory, NICS values of –8.9 and 28.8 ppm were obtained for benzene and cyclobutadiene, respectively. These controls are in good agreement with literature values of –9.7 and 27.6 ppm (HF/6-31+G(d)).[19] As described in the text, an NICS value of –19.4 ppm is found at the geometric center of the seven-membered ring of **TS3** (Figure S20). A NICS value of –19.4 ppm reveals a significant diatropic ring current. Thus, **TS3** is characterized as aromatic.[19]

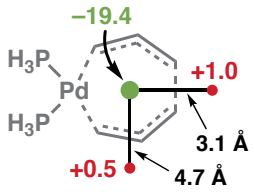

Figure S20. NICS calculated at various points along the plane in which the seven-membered ring of **TS3** resides.

Intrinsic Bonding Orbital Analysis

Analysis of the net flow of electron density through the Pd-catalyzed [π2s + π2s + σ2s + σ2s] pericyclic reaction was carried out by Intrinsic Bonding Orbital (IBO) analysis.[20] IBO analysis was carried out along the IRC describing **1** → **TS1** → **2**. SCF densities were obtained at the M06/def2-TZVP/CPCM(THF) level of theory and on BP86-D3(BJ)/LANL2TZ(f)[Pd]–6-31G(d) geometries, consistent with reference 13. Localization of the SCF density, frame alignment, and calculation of IBO displacement were carried out with the IBOView program.[21] For further details of this procedure and additional discussion of the relevant theory, see the seminal reports of Knizia and coworkers.[20] Note that results are largely independent of choice in density functional, and qualitatively identical results may be obtained with densities from an ab initio wavefunction method.

Coordinates of Optimized Structures

1 (from reference 13):

Pd	3.26950843604510	9.76495175299426	21.00419457583790
P	4.88760379688076	9.91056143608204	22.52617853020251
O	1.76323089045818	9.85273395150916	19.56727544961257
N	4.73672077332216	10.54415332504924	19.63123718078958
C	5.66479716159015	11.58043266656630	22.37210655628401
C	6.05286776841761	12.28298227144990	23.52750210444541
H	5.88044346623243	11.82935278494911	24.50705137912432
C	6.65502707296398	13.54760121695888	23.44624823669792
H	6.94006550973100	14.07152046747479	24.36423644109913
C	6.89414150294726	14.12910917932956	22.19424064883262
H	7.36371961850387	15.11462856551206	22.11935991477293
C	6.52949531405581	13.44156355992346	21.03130283255324
H	6.71323922845150	13.87918586505401	20.04749317569378
C	5.91009859557560	12.17592995841910	21.09953109400620
C	4.49621148079386	9.76586128277550	24.30762889493065
C	5.12573133223182	8.82710859888075	25.14580093157923
C	3.45590693711213	10.57164900582749	24.82053068256393
C	6.29779064189354	8.76383604753914	22.26744745932536
C	8.66169191708101	8.28093487949923	21.95189129910073
C	7.63576535709550	9.19902316151298	22.22341950025806
H	7.87325732712447	10.25431421205814	22.38831736338143
C	1.58241148549900	11.02631471877723	17.51134963414896
C	1.47195730710228	12.31523694111276	16.72287231157369
C	1.29849235553325	13.57134345806962	17.59270767032353

C	2.20906744918311	13.50486731690466	18.82587500043443
H	3.26531289202085	13.40315993290202	18.50141914943214
H	2.14624966749978	14.43727428164700	19.41761424495447
C	1.82359468325013	12.29371346547166	19.68308398030360
H	2.55333448148556	12.13753501363801	20.50301557428847
H	0.84928814927450	12.47477558523721	20.18302482740430
C	1.73167499679114	11.00121732300634	18.87697298656825
C	1.49457185141478	9.75071568180307	16.71544060807573
H	0.49077882104206	9.61383527184904	16.26234797065140
H	1.69102250022378	8.87873312148177	17.35968880892329
H	2.21397743291877	9.74376290392780	15.86788628761892
C	1.82915786962066	8.93256276815405	22.23151323449021
H	1.89049733374997	9.30935738238343	23.26436409134669
H	0.90406472498266	9.25359705043085	21.72957898501449
C	2.09319963673235	7.48510683052055	22.12472463706674
H	1.83540561644794	7.02146901941782	21.16107947340613
C	2.64311364824027	6.70730064271308	23.09189653994621
H	2.90762680928226	7.12067097449099	24.07262177128419
H	2.82860859695204	5.63889024188339	22.93702542209656
O	6.19166281413700	12.01280597861536	18.71732308070533
C	5.56708897833342	11.52327859032996	19.82455615481979
C	4.79194013712495	10.14827787682043	18.20161644670126
C	5.57520241933480	11.32567497108784	17.57675632938724
H	4.91112467256001	12.05035377293644	17.07678738998792
H	6.39053679122207	11.03368849230939	16.89974947561382
C	5.41718257874618	8.73504315551870	18.00408414001768
H	3.75774421412525	10.13907926776809	17.82656552699593
C	6.85149092773487	8.67654479772681	18.55985242808422
H	7.27553757736611	7.66731714949206	18.41879125500943
H	6.86856743909342	8.89352007186076	19.63934909696724
H	7.52399822575393	9.39222980540689	18.05226449971651
C	4.53539314928156	7.69089676370638	18.71641267414561
H	4.94051312171359	6.67568683559995	18.55430069922119
H	3.49877988107736	7.72374371413501	18.34067483091555
H	4.49243137279576	7.87671477084974	19.80394619549529
C	5.41423826388735	8.42950294389303	16.49131592164270
H	6.06277712373666	9.11872092045825	15.92037980261030
H	4.39260016842658	8.49606540548781	16.07646930602692
H	5.78778750915385	7.40587407418682	16.31265593443035
C	5.99347087068581	7.40317047970344	22.05123957983136
C	7.02404105774907	6.49024883574242	21.79375551863943
C	8.35763202052763	6.92832633213497	21.73505992516174
H	9.70011731504658	8.62525648356685	21.90636810454922
H	9.15978327879321	6.21530764070771	21.51810133401737
H	4.94779772396009	7.07289497365211	22.09059722957732
H	6.78358388324544	5.43545451333298	21.62521701567122

C	4.72030731309721	8.69788210776159	26.48339737109613
C	3.69435736062084	9.50787308352162	26.99208976486263
C	3.06644531886547	10.45020259861152	26.15949875396680
H	2.95495457680878	11.28867171860542	24.16056178932473
H	3.37889915788328	9.40295709349443	28.03517512713574
H	2.26100184380325	11.08007924779594	26.55059800289344
H	5.92701899392818	8.19644533883680	24.75026943723703
H	5.21028130174062	7.96150117146977	27.12877123500411
H	0.63043004853618	12.24663180626808	16.00089762427773
H	2.37806799098562	12.43371062029024	16.08235893827716
H	0.24775241185730	13.63629620569583	17.93689838934686
H	1.49649772850582	14.48135627543095	16.99591621019111

TS1 (from reference 13):

Pd	3.84257460521667	10.46200030588772	20.67075436643298
P	5.15074034163713	10.15540810514023	22.44989358148340
O	3.10449122326373	11.10540713618474	18.73383187122506
N	5.84104531506366	10.78626216728257	19.66415109109233
C	6.40986318662365	11.49163600998721	22.59047962762167
C	6.71682422964359	12.04545318851498	23.84936121116300
H	6.20191758410556	11.66365854261842	24.73492008858182
C	7.67509072661005	13.05776618909766	23.99055088860824
H	7.89438558298250	13.46131444642498	24.98454035117295
C	8.35744999100930	13.53799269390182	22.86256948398570
H	9.11203179215067	14.32442565264521	22.96182636562786
C	8.06577304234885	13.00824271948597	21.60222109516002
H	8.58223739357375	13.37829443471840	20.71372535693700
C	7.09404141793846	11.99557597485309	21.44104759074771
C	4.47514479813729	10.01649408498777	24.14915082829500
C	4.90739045080366	9.04920912519858	25.07773803637211
C	3.44234466375550	10.90972550080610	24.50663230633511
C	6.19029542302571	8.64574104111240	22.27853065557956
C	8.32212207053690	7.46608060877630	22.31920856089274
C	7.57839807602744	8.64027827139748	22.51455931926415
H	8.07733357196175	9.55767031783308	22.84136153335676
C	0.88636924621206	10.92433996852201	17.97358995934897
C	-0.35250497908573	11.67131799174944	17.49039565174745
C	-0.65337466383279	12.96706441495538	18.26385197996850
C	0.61409879139738	13.81639296880220	18.43802216049653
H	1.00255549452595	14.10471944398356	17.44117647855183
H	0.38461961013094	14.75587126803808	18.97421913413459
C	1.69022936022627	13.01569230648428	19.19003126954549
H	2.65114576969032	13.55754838041684	19.24166668484575
H	1.36966394196727	12.85589376641623	20.24273678516854
C	1.95194401964328	11.65649774255665	18.56198722310843

C	1.24369971788827	9.68062124272109	17.18569062379161
H	0.34785135653868	9.06384708940188	16.98870009423725
H	1.97977754912762	9.07570288425797	17.73671398114214
H	1.68764089912940	9.94423269215636	16.20571411840790
C	1.97995551424616	9.99043034672134	21.56835818584344
H	2.27504508408442	9.33148410062073	22.39883360717235
H	1.57104379778184	10.94641581615323	21.94185872745719
C	1.20753320361223	9.36862043951070	20.53106867229126
H	1.43547267909753	8.32307376391354	20.28400190467620
C	0.22286470620963	10.03201990852669	19.77898145302082
H	-0.20639528570615	10.94379297084639	20.21273301917761
H	-0.49507347432973	9.42165325119865	19.21830890218480
O	7.70735402531856	11.95524235298889	19.11611308360739
C	6.82458843816749	11.52867208669833	20.07380180945096
C	6.00170237925380	10.55066214014787	18.21280281103999
C	7.15565812499212	11.51510437144334	17.83698124274905
H	6.80683245334326	12.41245487571676	17.29844119185316
H	7.97769986227431	11.04789514174991	17.27374738516654
C	6.25997159415831	9.04286903872788	17.90763591380394
H	5.05350058107962	10.84098597742140	17.73124894497424
C	7.49998144665082	8.53204749400017	18.66392303280958
H	7.67519822345439	7.46604056528939	18.43635155343050
H	7.36214836253402	8.62341059270417	19.75291686086506
H	8.41523401893656	9.08554073829311	18.38378840056377
C	5.01874592008928	8.23644334593780	18.33502313167518
H	5.17039827794867	7.16041938571676	18.13366252912862
H	4.12302877614314	8.57772334224015	17.78952498466234
H	4.81413185620666	8.36689778224057	19.41158947170407
C	6.45205590061290	8.88219978223940	16.38547314945966
H	7.35738938507715	9.39791225610909	16.01676639824987
H	5.58168142946780	9.27880830319676	15.83155730512140
H	6.55728026995629	7.81347868903979	16.12772874347014
C	5.55551924218644	7.45855655031138	21.85765497066307
C	6.29785227830335	6.28496713831961	21.67608903859047
C	7.68469808580988	6.28865019089804	21.89943948632574
H	9.40334170633804	7.47349295584421	22.49300312790627
H	8.26807865874872	5.37561151820832	21.74161781951342
H	4.47882059562402	7.47216971085428	21.65635776451643
H	5.79633528111831	5.37028095240347	21.34351483996044
C	4.32162749818138	8.98589598305703	26.35063244758296
C	3.30538648461203	9.88696100052709	26.70625692807196
C	2.86842497231517	10.85126943140725	25.78309331379914
H	3.09636306714269	11.64514044448267	23.77203228602484
H	2.84903740792217	9.83366078032276	27.70019750765648
H	2.06985055518909	11.54981724844311	26.05378061296737
H	5.70408672893973	8.35136333434521	24.80241273274088

H	4.66229480830661	8.23184365038084	27.06813086331798
H	-1.22988158897917	10.99493691410892	17.52676898919124
H	-0.21370820011031	11.91466999070673	16.41462979114665
H	-1.05964475087292	12.72013348770468	19.26364707405090
H	-1.44082198141107	13.53971118096474	17.73992763593413

2 (from reference 13):

Pd	3.40892821984617	9.57548180994135	20.63708137423307
P	4.84593533321281	9.79648201908891	22.39467584511297
O	3.72121715500973	12.10929642182155	17.76164834581262
N	5.19863442987848	10.22736089300746	19.45410200953097
C	5.60750763629421	11.48086667325468	22.25115597994107
C	5.69592805542466	12.32728514020735	23.37125677904141
H	5.32772089945508	11.96915954521793	24.33629927115776
C	6.24850212031137	13.61395298205514	23.27742444546726
H	6.29458925032951	14.24978402392602	24.16778885514220
C	6.74570177325324	14.07368666891647	22.05149476088817
H	7.18524188860840	15.07248156009153	21.96753037224923
C	6.67389926572365	13.24677006445060	20.92410559721537
H	7.05018617831925	13.59074590141271	19.95801111939930
C	6.09639667958848	11.96160478637347	20.99991108123387
C	4.29513244063977	9.74735606637389	24.14941702044027
C	5.14207640491821	9.40414709839555	25.22237129427582
C	2.94700565201092	10.07018704440548	24.40379135034721
C	6.33013870592848	8.70490264048157	22.41219925611539
C	8.73168119807324	8.28782974203697	22.45055158685528
C	7.65130966727384	9.18225825123993	22.51114826416465
H	7.83483884037841	10.25512305831720	22.62467765182594
C	1.39933668244652	11.51472730954684	18.13004322753791
C	0.48499025360100	12.77550794929948	17.94808873920420
C	0.42350108471802	13.67901939931408	19.19370299302099
C	1.82642350144789	14.11638424814738	19.64954862904691
H	2.26451189638659	14.78916718009596	18.88646478918058
H	1.77194646060617	14.69352923408393	20.59046380508886
C	2.77756911872315	12.90332008504502	19.82980940627712
H	3.80816342495517	13.23311445389370	20.03229499853076
H	2.45038247666115	12.26767578640207	20.67419431516601
C	2.76140977289175	12.10160311216322	18.53758653275498
C	1.52240375586956	10.76175437906711	16.79980764244113
H	0.53039228107476	10.40472449743852	16.46973016897448
H	2.18686008071839	9.88782162542038	16.90595243188864
H	1.94802984330979	11.40849203966424	16.01581701515308
C	1.46660664872501	8.85307474989263	20.92932340384906
H	1.53083638359487	7.77645428264424	21.14017539338617
H	0.88606648516123	9.41788749921577	21.67370453060018

C	1.52997925447675	9.33027251887933	19.58362570519831
H	1.64878434054261	8.59259858774980	18.77748582148616
C	0.77917867217335	10.59848756547767	19.21686884553761
H	0.62030860044023	11.17536312387277	20.14451125661726
H	-0.23873947905966	10.33398893689353	18.85210778438655
O	6.87215517631868	11.58773394657944	18.75910791431981
C	6.01419130441858	11.19327446281953	19.74224560238274
C	5.48851682565873	9.77007793739730	18.07594119280332
C	6.48555146618170	10.84111168931777	17.56209155743612
H	6.00935805072447	11.55154279054394	16.87143550329406
H	7.41052027828996	10.43653577587442	17.12460728172655
C	6.00706941297575	8.30099776483311	18.03487590543506
H	4.54514993142261	9.82813557169816	17.50833320716369
C	7.30630727234765	8.15561854093982	18.84813395892141
H	7.65472811202569	7.10838876048460	18.83012573012424
H	7.14663609546928	8.43649850823804	19.90018662676940
H	8.12132855259047	8.78247423870561	18.44337346725440
C	4.92737419174689	7.36453617069685	18.61013298179947
H	5.27460562116382	6.31566206669788	18.58154134734334
H	3.99083647535687	7.43388370644379	18.02764214036510
H	4.68399855429023	7.62727690917917	19.65654513345953
C	6.25428639366204	7.92296878203579	16.55943986291501
H	7.04960296746653	8.53506308192094	16.09691355095989
H	5.33553865712328	8.04621797448163	15.95716203214114
H	6.56807200182852	6.86669279909721	16.48534828251532
C	6.10679548203821	7.31973759245566	22.26031096784333
C	7.18532401305821	6.42811630404683	22.21664707292259
C	8.50166334527760	6.91162392553700	22.30464252496925
H	9.75620499363189	8.66935285771535	22.51650253636760
H	9.34623123455324	6.21668185440797	22.25279215210035
H	5.07928406586081	6.95345092337835	22.15759579277393
H	7.00055967907282	5.35557066507219	22.09580205013044
C	4.64536242375417	9.39396093181183	26.53394442652993
C	3.30515824219112	9.73205368959254	26.78323383551776
C	2.45669242550519	10.07192375755660	25.71683866553102
H	2.29478305017913	10.30414991516969	23.55440270148741
H	2.91998514745839	9.72198750638516	27.80835325948386
H	1.40850384670283	10.32532367512722	25.90795941032653
H	6.18737959396861	9.14408159613316	25.02589897379470
H	5.30593825060969	9.12155781691829	27.36411005272814
H	-0.52951949829738	12.43323246967131	17.66630218325726
H	0.87227257305116	13.36229073369384	17.09177376839953
H	-0.08649513997127	13.15005829272420	20.02007640010707
H	-0.19370328510800	14.56928102095648	18.97153032362477

Diallyl sulfone **3** (CASSCF geometry):

S	0.35747064753576	12.04890784237913	4.45274609365606
C	0.96921359870812	10.35332225159514	4.61292125419759
C	-0.08715957591369	9.35937358010859	4.98894587084294
H	1.71660251981265	10.45651986571805	5.39248548790718
H	1.47023566550203	10.10504567836464	3.68793210067471
C	-0.37569456851365	8.27640345461669	4.26574080469331
H	-1.12576826008149	7.57845951982901	4.58701436746332
H	0.13695675315403	8.05269393925871	3.34734241030587
H	-0.61496133549215	9.55456425714884	5.90456133176481
C	-0.75518609814300	12.05369868601239	3.02555670720221
C	-0.06709421972976	11.80454375966122	1.71800029078483
H	-1.17608789996819	13.05252931988143	3.07180842896953
H	-1.54109383078097	11.34036899976275	3.22995624329985
C	-0.39300575416324	10.81342917733471	0.88699129827062
H	0.11298812785410	10.68749972715153	-0.05165930004415
H	-1.17869035457970	10.11547674786058	1.11475228689372
H	0.72113345536332	12.48846056253122	1.46113322243422
O	1.46868159647423	12.86412832143325	4.14244545328683
O	-0.42613846703837	12.33948330935167	5.59168564739645

TS5 (CASSCF geometry):

S	0.40085373117997	12.19514996865006	4.56243209615286
C	0.91027586429646	10.46505387129021	4.82271532843759
C	-0.12912939901855	9.44995618957432	4.46381421138742
H	1.15787087489592	10.45432919005805	5.87745783009860
H	1.81699014867493	10.33207155825919	4.25045162451345
C	-0.11446125662132	8.88683004225812	3.14375309601298
H	-0.77526753872419	8.04354622157732	3.01510864046526
H	0.87830739409482	8.65363613826484	2.78898130694913
H	-1.03410077332474	9.43825159455407	5.04356860032879
C	-0.60577926605623	12.24697923617163	3.04435628317084
C	-0.13846247770467	11.33156308662311	1.95660009354837
H	-0.54670035735281	13.29207634242614	2.76475573353949
H	-1.61787528473193	12.02463366444052	3.35017400196510
C	-0.70921529253207	10.01754814028603	1.87007274456733
H	-0.45642500708716	9.48399444501731	0.96687879616239
H	-1.77558510104928	10.00222058608154	2.03875779389005
H	0.82180427909187	11.53098771207896	1.51690591942578
O	1.58050218756863	12.93744054538528	4.32249226481139
O	-0.45120072559964	12.55864046700272	5.63108363457301

Diradical **10** (CASSCF geometry):

S	0.40818342766984	12.21983658625659	4.58086526286423

C	0.88697170113672	10.47512478850876	4.83910877206008
C	-0.13368816289347	9.46931706656585	4.42658595997658
H	1.08913318758774	10.44702527675920	5.90298143144850
H	1.81576781977008	10.34885835482377	4.30059308486550
C	-0.11849822643917	8.93290843400189	3.03409046368845
H	-0.68609511589835	8.01139082002527	2.98046604074867
H	0.90268449770751	8.70322062420846	2.74569596415096
H	-1.02855738482656	9.38857902689503	5.01574136055925
C	-0.57696962867412	12.25562241863942	3.04198907317169
C	-0.13742547320814	11.30022682403919	1.98482730540029
H	-0.48125812648989	13.28901237437917	2.73145985088398
H	-1.59724654475578	12.07315038531079	3.34914304141054
C	-0.71865613429103	9.92630775850911	1.94576357006448
H	-0.55702276891353	9.47774142366594	0.97267599888034
H	-1.79129815985545	9.98232585169672	2.10401367189011
H	0.79179517818118	11.49689779443476	1.48254934534303
O	1.59959484267134	12.94732506697431	4.35799023383020
O	-0.45501292847894	12.60003812430470	5.63381956876279

TS6 (CASSCF geometry):

S	0.58426048914877	12.35495876344218	4.50347475798360
C	0.76563392818988	10.18130486682548	5.09195481162345
C	-0.15998594651248	9.42240209794968	4.37620513782028
H	0.59656636250199	10.32883890722220	6.14403145178944
H	1.80070744840580	10.13126947297771	4.80054656995029
C	0.03424635958173	8.98307361572213	2.94693633743267
H	-0.31044705558072	7.95965726376298	2.83005317355078
H	1.08957666995150	8.99981423159535	2.69437466840319
H	-1.14674283923322	9.30090464306342	4.79030428136334
C	-0.66944297370226	12.25927638132190	3.04486125557884
C	-0.29590719873958	11.33734568348633	1.98731594397224
H	-0.64482572990182	13.29879784264573	2.74391660126243
H	-1.60237765951219	12.02773299958368	3.53861415339258
C	-0.74655906850946	9.89843176778375	1.95273298187086
H	-0.62878459206258	9.51017894972555	0.94726449698275
H	-1.80620424055789	9.84520559164440	2.19206353014569
H	0.51176020755485	11.62974754427105	1.34217697505237
O	1.83900613209864	12.73824254004445	3.98013149055667
O	0.00192170687902	13.13772583693040	5.52340138126805

Sulfur dioxide **4** (CASSCF geometry):

S	-3.62364112086088	9.99412265880031	1.57930579067120
O	-4.70117577514101	10.86278979112046	1.74069720788480
O	-2.32783410399810	10.50543855007923	1.61323700144401

1,5-hexadiene **5** s-*trans* conformer (CASSCF geometry):

C	-15.79671254844809	19.62784833183823	2.98404282113774
C	-16.10854780484172	18.62372954787715	3.80481048989501
H	-15.57191840555579	18.45634844093010	4.72208513253682
H	-16.90619760233716	17.94066568548304	3.57828494789632
C	-14.70330151353748	20.63180019144333	3.22396409188588
H	-16.36713246182979	19.75459070776224	2.07729946757165
C	-15.22949687368783	22.06944426044722	3.32242535116545
H	-13.98427289180937	20.57489476171194	2.40970332485138
H	-14.16723501076640	20.37971289090769	4.13280289045238
C	-14.13011201653164	23.07987992362649	3.49963412871804
H	-15.93071462528147	22.14236719157724	4.14697388305967
H	-15.78466885638515	22.30410778163848	2.41689961115932
C	-13.99647089722293	23.89040246042062	4.55051422699967
H	-13.18388120807869	24.58966271626021	4.62028707302750
H	-14.69808713180210	23.87857246770140	5.36597415688129
H	-13.39806015188434	23.12870364037456	2.70884840276185

1,5-hexadiene **5** s-*cis* conformer (CASSCF geometry):

C	-15.68653976135932	19.53485254034207	2.91030345122271
C	-16.07556505807565	18.49759654443785	3.65259105748023
H	-15.72746407734631	18.36209569363375	4.66146581224672
H	-16.75301135350131	17.75664839380491	3.27033741630101
C	-14.73606936898643	20.60945797614487	3.35432251631976
H	-16.06844425656496	19.62665054639524	1.90575656337581
C	-15.32376994067612	22.05287842299805	3.23202190863941
H	-13.83765512477437	20.56585731554495	2.74424012383432
H	-14.43015873003113	20.43251269217485	4.38071990170875
C	-16.47597470048769	22.31219780864149	4.15967469480827
H	-15.62793820321127	22.23047289141857	2.20522192412983
H	-14.52352050888237	22.75480501251457	3.45137026514254
C	-17.68490754794102	22.73238359195972	3.78534628159811
H	-18.46491452136203	22.90809143128789	4.50282868024500
H	-17.92672751931311	22.91121164147045	2.75244034263189
H	-16.28632932748670	22.14385749723047	5.20804906031558

Complex **6** (DFT geometry):

Pd	0.07927074507815	12.24034209215000	4.78411487578694
C	0.98737624049873	10.47646607889792	4.04983068535827
C	2.44042841844212	10.54902689906720	4.22629879054284
H	0.71087825698903	10.40787755416243	2.99840450241430
H	0.54566747387074	9.64032251554081	4.59975977259049

C	3.17662577961688	9.84159617958571	5.09058883555017
H	4.24780890534539	9.98346219240712	5.17233966173592
H	2.73134801748205	9.07581996188833	5.71889764028128
H	2.95871163764078	11.27331721591301	3.59835875875198
C	-0.79324085380584	12.44442649771748	2.87333634375677
C	-1.94149070267777	11.53341106414385	2.86434867716505
H	-0.00966429106172	12.15628410817079	2.17256211095283
H	-1.09546173546794	13.47322200707576	2.65443780311373
C	-3.22934939335106	11.88770445980430	2.86670559139197
H	-4.02093367191159	11.14865339337686	2.89366506031577
H	-3.53058322129562	12.93072270943176	2.82746785583406
H	-1.70572752994073	10.47042058202333	2.88533307434274
P	1.09346684459823	11.85552288337293	6.81222582254403
H	0.55186857467733	12.34191645956828	8.02682485359925
H	2.40201811674024	12.34934530548531	6.98830787448621
P	-1.07989145466214	14.14898132118945	5.28314080492867
H	-0.73606625002045	15.33916581156848	4.60491672654225
H	-1.23538212746898	14.72404685299512	6.56754049077189
H	-2.44541651098712	14.11464659351614	4.93066677937947
H	1.33363873167130	10.52912926094729	7.22294660786298

TS3 (DFT geometry):

Pd	0.01113171305548	12.21034771325277	4.97185032297384
C	0.77225811597929	10.15236816099254	4.68440370282270
C	-0.37432481351280	9.38428327903291	4.34750276050131
H	1.16612083673174	9.94412653997201	5.67851117699016
H	1.56393235397139	10.16565008802084	3.93660486351538
C	-0.60121222050714	8.85879934033455	3.10227283449459
H	-1.45229322131086	8.20879942613711	2.93663486261553
H	0.23673208033970	8.71666867730399	2.43269389153903
H	-1.13363402189388	9.25053756002476	5.11490928693610
C	-0.89083686152788	12.48872498528177	2.94801589121881
C	-0.55230603276640	11.51891184426245	1.98257840485364
H	-0.40035653781427	13.45523823816321	2.82207401895074
H	-1.95786942205163	12.58125543512562	3.14641523888302
C	-1.32370255834951	10.42557827414071	1.69928705206514
H	-1.09064028669049	9.79193104223490	0.85324367660134
H	-2.34984155928286	10.39379939465763	2.04875907271849
H	0.43327966408528	11.58615368174376	1.52587085810883
P	1.45982983271885	12.23844373014170	6.76221476344352
H	1.73106129723849	13.35453493879111	7.59373169429537
H	2.80996390752327	11.89290266161511	6.51904896618760
P	-1.29019313610133	14.02900454710556	5.55725279918838
H	-1.98975955039876	14.78899946729273	4.58758757291786
H	-0.79745476198389	15.13368438256653	6.29475911975046

H	-2.40169829440476	13.78959376964220	6.40063999653779
H	1.26292447695297	11.31429182216338	7.81641917189033

Complex **8** (DFT geometry):

Pd	0.657933000	11.679009000	4.737666000
C	1.698178000	9.876625000	4.157083000
C	0.333515000	9.623995000	4.051212000
C	-0.330974000	9.442738000	2.713570000
C	-2.844675000	12.267528000	2.457843000
C	-1.769891000	11.498986000	2.332836000
C	-1.733807000	10.017557000	2.557662000
P	-1.323849000	12.569977000	5.450213000
H	-1.823696000	13.786824000	4.932171000
H	-1.392156000	12.962762000	6.811908000
P	2.283511000	13.247625000	5.049504000
H	3.609515000	12.914471000	5.422062000
H	2.181821000	14.342637000	5.944597000
H	2.660053000	14.036369000	3.934902000
H	-2.568254000	11.895682000	5.437174000
H	0.312537000	9.862698000	1.932192000
H	-0.379655000	8.364366000	2.513602000
H	-2.352512000	9.752555000	3.421935000
H	-2.204777000	9.536054000	1.691810000
H	2.254462000	9.573888000	5.038302000
H	2.291243000	10.021748000	3.258807000
H	-0.164990000	9.128616000	4.882214000
H	-0.839156000	11.951142000	1.993226000
H	-3.796908000	11.865959000	2.792237000
H	-2.812845000	13.326388000	2.229180000

Complex **7** (DFT geometry):

Pd	0.380448000	12.744188000	4.779333000
O	1.892361000	11.900846000	3.692626000
C	2.251072000	10.683518000	3.993171000
C	1.639877000	9.801885000	4.809921000
H	2.069076000	8.821132000	4.966648000
H	0.668336000	10.012649000	5.247214000
H	3.182102000	10.374345000	3.503113000
C	-0.635097000	12.896518000	2.967200000
C	-1.256627000	11.585853000	2.764604000
H	0.229088000	13.074301000	2.326707000
H	-1.351176000	13.718607000	2.887939000
C	-2.570655000	11.353016000	2.724079000
H	-2.965296000	10.352750000	2.592587000

H	-3.292880000	12.161263000	2.800424000
H	-0.570130000	10.747830000	2.665201000
P	1.683456000	12.411023000	6.708921000
H	1.867871000	13.496400000	7.599412000
H	3.031847000	12.069456000	6.509617000
P	-1.405236000	13.742036000	5.588077000
H	-1.689776000	15.063770000	5.183968000
H	-1.623300000	13.913976000	6.973713000
H	-2.634090000	13.138571000	5.250521000
H	1.345167000	11.448996000	7.681815000

TS4 (DFT geometry):

Pd	-0.42148010307612	12.28899351558105	5.05611409811586
O	-0.33619048955232	10.09867979358262	5.20609987120670
C	-0.86923018864008	9.27995418789769	4.39162673609982
C	-0.22561902031017	8.73590931428709	3.31105378975747
H	-0.70184378250186	7.94853193754419	2.73936674824975
H	0.84553161636951	8.86027431410283	3.21099342441497
H	-1.94758530314093	9.07613137569856	4.49874175688810
C	-1.41993821436898	12.46250460969018	3.18294361293458
C	-0.51845548088304	11.69452106765484	2.38391582401475
H	-1.46280328531489	13.52260948059490	2.93475269149549
H	-2.41831042423060	12.04080848757141	3.30314501709100
C	-0.79329684057973	10.43442785577553	1.91384559090135
H	-0.13962331560175	9.98102392974632	1.17943431793478
H	-1.81349641639443	10.07382367181423	1.91692407591945
H	0.43907696749224	12.14203168082447	2.13092514043255
P	1.11667665599999	11.80054875973404	6.81502225150353
H	1.80302143255638	12.69905059463158	7.66910247239854
H	2.23063189066872	11.00919622467464	6.46565740162336
P	-0.92711892390812	14.42601859349280	5.33445694675466
H	-2.26948429316828	14.84792103508812	5.18845751337222
H	-0.37143835265767	15.36107593095086	4.43039026276634
H	-0.64554764017274	15.15348553886600	6.51548690427186
H	0.60652451141489	10.95903110019524	7.82436455185259

Complex **9** (DFT geometry):

Pd	0.620551000	11.665836000	4.708215000
C	1.696455000	9.886430000	4.136185000
C	0.337627000	9.610350000	4.006925000
C	-0.308627000	9.439800000	2.659423000
O	-2.795237000	12.109777000	2.661298000
C	-1.805237000	11.458521000	2.448569000
C	-1.730314000	9.962832000	2.560176000

P	-1.328150000	12.659139000	5.393693000
H	-1.788027000	13.845189000	4.779886000
H	-1.331890000	13.155154000	6.720006000
P	2.261354000	13.216380000	5.083376000
H	3.557119000	12.859212000	5.530186000
H	2.130867000	14.323782000	5.958431000
H	2.709114000	13.979585000	3.978248000
H	-2.595380000	12.034386000	5.457779000
H	0.308458000	9.929778000	1.897040000
H	-0.307092000	8.372619000	2.405346000
H	-2.353211000	9.640936000	3.399011000
H	-2.213911000	9.576462000	1.652550000
H	2.243675000	9.579074000	5.021307000
H	2.301209000	10.049600000	3.248778000
H	-0.166116000	9.098778000	4.824825000
H	-0.872408000	11.948189000	2.088728000

References

(1) (a) Neese, F. The ORCA Program System. *Wiley Interdisciplinary Reviews: Computational Molecular Science* **2012**, 2, 73–78. (b) Neese, F. Software Update: The ORCA Program System, Version 4.0. *Wiley Interdisciplinary Reviews: Computational Molecular Science* **2018**, *8*, e1327.

(2) Weigend, F.; Ahlrichs, R. Balanced Basis Sets of Split Valence, Triple Zeta Valence and Quadruple Zeta Valence Quality for H to Rn: Design and Assessment of Accuracy. *Phys. Chem. Chem. Phys.* **2005**, *7*, 3297–3305.

(3) Adamo, C.; Barone, V. Toward Reliable Density Functional Methods without Adjustable Parameters: The PBE0 Model. *J. Chem. Phys.* **1999**, *110*, 6158–6170.

(4) (a) Grimme, S.; Antony, J.; Ehrlich, S.; Krieg, H. A consistent and accurate *ab initio* parametrization of density functional dispersion correction (DFT-D) for the 94 elements H-Pu *J. Chem. Phys.* **2010**, *132*, 154104. (b) Grimme, S.; Ehrlich, S.; Goerigk, L. *J. Comput. Chem.* **2011**, *32*, 1456–1465. (c) Becke, A. D.; Johnson, E. R. A density-functional model of the dispersion interaction. *J. Chem. Phys.* **2005**, *122*, 154101. (d) Johnson, E. R.; Becke, A. D. A post-Hartree–Fock model of intermolecular interactions. *J. Chem. Phys.* **2005**, *123*, 024101. (e) Johnson, E. R.; Becke, A. D. A post-Hartree-Fock model of intermolecular interactions: Inclusion of higher-order corrections. *J. Chem. Phys.* **2006**, *124*, 174104.

(5) Andrae, D.; Häußermann, U.; Dolg, M.; Stoll, H.; Preuß, H. Energy-Adjusted ab Initio Pseudopotentials for the Second and Third Row Transition Elements. *Theoret. Chim. Acta* **1990**, *77*, 123–141.

(6) (a) Angeli, C.; Cimiraglia, R.; Evangelisti, S.; Leininger, T.; Malrieu, J.-P. Introduction of N-Electron Valence States for Multireference Perturbation Theory. *J. Chem. Phys.* **2001**, *114*, 10252–10264. (b) Angeli, C.; Cimiraglia, R.; Malrieu, J.-P. N-Electron Valence State Perturbation Theory: A Fast Implementation of the Strongly Contracted Variant. *Chemical Physics Letters* **2001**, *350*, 297–305. (c) Angeli, C.; Cimiraglia, R.; Malrieu, J.-P. N-Electron Valence State Perturbation Theory: A Spinless Formulation and an Efficient Implementation of the Strongly Contracted and of the Partially Contracted Variants. *J. Chem. Phys.* **2002**, *117*, 9138–9153.

(7) Nakano, H. Quasidegenerate Perturbation Theory with Multiconfigurational Self-consistent-field Reference Functions. *J. Chem. Phys.* **1993**, *99*, 7983–7992.

(8) Marenich, A. V.; Cramer, C. J.; Truhlar, D. G. Universal Solvation Model Based on Solute Electron Density and on a Continuum Model of the Solvent Defined by the Bulk Dielectric Constant and Atomic Surface Tensions. *J. Phys. Chem. B* **2009**, *113*, 6378–6396.

(9) Grimme, S. Supramolecular Binding Thermodynamics by Dispersion-Corrected Density Functional Theory. *Chemistry – A European Journal* **2012**, *18*, 9955–9964.

(10) Neese, F.; Wennmohs, F.; Hansen, A.; Becker, U. Efficient, Approximate and Parallel Hartree-Fock and Hybrid DFT Calculations. A 'Chain-of-Spheres' Algorithm for the Hartree-Fock Exchange. *Chemical Physics* **2009**, *356*, 98–109.

(11) Stoychev, G. L.; Auer, A. A.; Neese, F. Automatic Generation of Auxiliary Basis Sets. *J. Chem. Theory Comput.* **2017**, *13*, 554–562.

(12) Woodward, R. B.; Hoffmann R.; *The Conservation of Orbital Symmetry*; Verlag Chemie GmbH (BRD) and Academic Press Inc. (USA), 1971.

(13) Cusumano, A. Q.; Stoltz, B. M.; Goddard, W. A. III Reaction Mechanism, Origins of Enantioselectivity, and Reactivity Trends in Asymmetric Allylic Alkylation: A Comprehensive Quantum Mechanics Investigation of a $C(sp^3)$–$C(sp^3)$ Cross-Coupling. *J. Am. Chem. Soc.* **2020**, *142*, 13917–13933.

(14) For PBE see: (a) Perdew, J. P.; Burke, K.; Ernzerhof, M. Generalized Gradient Approximation Made Simple. *Phys. Rev. Lett.* **1996**, *77*, 3865–3868. For M06-2X see (b) Zhao, Y.; Truhlar, D. G. The M06 Suite of Density Functionals for Main Group Thermochemistry, Thermochemical Kinetics,

Noncovalent Interactions, Excited States, and Transition Elements: Two New Functionals and Systematic Testing of Four M06-Class Functionals and 12 Other Functionals. *Theor Chem Account* **2008**, *120*, 215–241.

(15) Heisenberg, W. Zur Theorie des Ferromagnetismus. *Z. Physik* **1928**, *49*, 619–636.

(16) Neese, F. Definition of Corresponding Orbitals and the Diradical Character in Broken Symmetry DFT Calculations on Spin Coupled Systems. *Journal of Physics and Chemistry of Solids* **2004**, *65*, 781–785.

(17) (a) Yamaguchi, K.; Takahara, Y.; Fueno, T. Ab-Initio Molecular Orbital Studies of Structure and Reactivity of Transition Metal-OXO Compounds. In *Applied Quantum Chemistry*; Smith, V. H., Schaefer, H. F., Morokuma, K., Eds.; Springer Netherlands: Dordrecht, 1986; pp 155–184. (b) (b) Soda, T.; Kitagawa, Y.; Onishi, T.; Takano, Y.; Shigeta, Y.; Nagao, H.; Yoshioka, Y.; Yamaguchi, K. Ab Initio Computations of Effective Exchange Integrals for H–H, H–He–H and Mn2O2 Complex: Comparison of Broken-Symmetry Approaches. *Chemical Physics Letters* **2000**, *319*, 223–230. (c) Ferré, N.; Guihéry, N.; Malrieu, J.-P. Spin Decontamination of Broken-Symmetry Density Functional Theory Calculations: Deeper Insight and New Formulations. *Phys. Chem. Chem. Phys.* **2015**, *17*, 14375–14382.

(18) (a) Miralles, J.; Castell, O.; Caballol, R.; Malrieu, J.-P. Specific CI Calculation of Energy Differences: Transition Energies and Bond Energies. *Chemical Physics* **1993**, *172*, 33–43. For discussion on the iterative method (IDDCI) see: (b) García, V. M.; Castell, O.; Caballol, R.; Malrieu, J. P. An Iterative Difference-Dedicated Configuration Interaction. Proposal and Test Studies. *Chemical Physics Letters* **1995**, *238*, 222–229.

(19) (a) Schleyer, P. von R.; Maerker, C.; Dransfeld, A.; Jiao, H.; van Eikema Hommes, N. J. R. Nucleus-Independent Chemical Shifts: A Simple and Efficient Aromaticity Probe. *J. Am. Chem. Soc.* **1996**, *118*, 6317–6318. For a general review of the concept and applications of NICS, see: (b) Chen, Z.; Wannere, C. S.; Corminboeuf, C.; Puchta, R.; Schleyer, P. von R. Nucleus-Independent Chemical Shifts (NICS) as an Aromaticity Criterion. *Chem. Rev.* **2005**, *105*, 3842–3888. For discussion on NICS analysis of transition states, see: (c) Schleyer, P. von R.; Wu, J. I.; Cossío, F. P.; Fernández, I. Aromaticity in Transition Structures. *Chem. Soc. Rev.* **2014**, *43*, 4909–4921. (d) Jiao, H.; Schleyer, P. von R. Aromaticity of Pericyclic Reaction Transition Structures: Magnetic Evidence. *Journal of Physical Organic Chemistry* **1998**, *11*, 655–662.

(20) (a) Knizia, G. Intrinsic Atomic Orbitals: An Unbiased Bridge between Quantum Theory and Chemical Concepts. *J. Chem. Theory Comput.* **2013**, *9*, 4834–4843. (b) Knizia, G.; Klein, J. E. M. N. Electron Flow in Reaction Mechanisms—Revealed from First Principles. *Angew. Chem. Int. Ed.* **2015**, *54*, 5518–5522. (c) Klein, J. E. M. N.; Knizia, G. CPCET versus HAT: A Direct Theoretical Method for Distinguishing X–H Bond-Activation Mechanisms. *Angew. Chem. Int. Ed.* **2018**, *57*, 11913–11917.

(21) Knizia, G. *IboView*; see http://www.iboview.org.